



Bergische Universität Wuppertal

Fachbereich Mathematik und Naturwissenschaften

Institute of Mathematical Modelling, Analysis and
Computational Mathematics (IMACM)

Preprint BUW-IMACM 12/32

Daniel Heubes, Andreas Bartel, Matthias Ehrhardt

**Characteristic Boundary Conditions in the
Lattice Boltzmann Method for Fluid and Gas
Dynamics**

December 13, 2012

<http://www.math.uni-wuppertal.de>

Characteristic Boundary Conditions in the Lattice Boltzmann Method for Fluid and Gas Dynamics

Daniel Heubes*, Andreas Bartel*, Matthias Ehrhardt*

*Bergische Universität Wuppertal, Fachbereich Mathematik und Naturwissenschaften,
Lehrstuhl für Angewandte Mathematik und Numerische Analysis, Gaußstrasse 20, 42119
Wuppertal, Germany*

Abstract

For numerically solving fluid dynamics problems efficiently one is often facing the problem that one has to confine the computational domain to a small domain of interest introducing so-called non-reflecting boundary conditions (NRBCs).

In this work we address the problem of supplying NRBCs in fluid simulations in two space dimensions using the lattice Boltzmann method (LBM): so-called characteristic boundary conditions are revisited and transferred to the framework of lattice Boltzmann simulations.

Numerical tests show clearly that the unwanted unphysical reflections can be reduced significantly by applying our newly developed methods. Hereby the key idea is to transfer and generalize Thompson's boundary conditions originally developed for the nonlinear Euler equations of gas dynamics to the setting of lattice Boltzmann methods. Finally, we give strong numerical evidence that the proposed methods possess a long-time stability property.

Keywords: Computational fluid dynamics, lattice Boltzmann method, unbounded domain, non-reflecting boundary conditions, characteristic boundary conditions, LODI.

2010 MSC: 65M06, 65M22, 65M25, 76D05

*corresponding author

Email addresses: heubes@math.uni-wuppertal.de (Daniel Heubes), bartel@math.uni-wuppertal.de (Andreas Bartel), ehrhardt@math.uni-wuppertal.de (Matthias Ehrhardt)

1. Introduction

For fluid simulations, the *lattice Boltzmann method* (LBM) has been proven to be a quite flexible tool [1, 2, 3] Its ease of implementation and its applicability to complex flows (including multicomponent flow, multiphase flow, obstacles, complex physical interaction such as fluid structure interaction) make this method extremely attractive for real-world simulations.

To enable an efficient numerical simulation, often a small bounded simulation domain is needed. Such a situation is obtained by confining the domain correspondingly. Thereby the physical boundaries are supplemented with some additional, artificial boundaries, where numerical conditions have to be assigned to the state variables. Ideally, these boundaries and these boundary conditions shall have no influence on the simulation result, i.e., the interaction of the artificial boundary with numerical quantities shall at least be below the discretization error of the interior scheme. This is exactly the aim of absorbing or *non-reflecting boundary conditions* (NRBCs).

Several studies have been made on NRBCs for direct solvers. Starting from the pioneering work for absorbing boundary conditions for wave equations by Engquist and Majda [4], *characteristic boundary conditions* (CBCs) in the field of nonlinear hyperbolic equations were developed by Hedstrom [5] and Thompson [6], which are non-reflecting. Kröner [7] derived approximate, exact absorbing boundary conditions for the linear Euler equations. Poinsoot and Lele [8] derived NRBCs for the Navier-Stokes equations.

In a different fully discrete approach Wilson [9] and later Rowley and Colonius [10] derived for the linear Euler equations the NRBCs directly for the chosen numerical scheme. This approach has the advantage that these discrete boundary conditions are already perfectly adapted to the interior scheme resulting in higher accuracy and better stability properties compared to the previous approaches. For a concise review article on absorbing boundary conditions for hyperbolic systems we refer the interested reader to [11]. We remark that a closely related question is the construction of so-called *far field boundary conditions* that are optimized to numerically approximate the stationary solution of the hyperbolic systems, cf. [12].

Let us emphasize that the situation of NRBCs for the LBM is completely different. Only few studies have been made on this subject, cf. [13] for a comparison of different approaches in an aeroacoustic application. Recently, Najafi-Yazdi and Mongeau [14] developed an absorbing layer boundary condition, based on the *perfectly matched layer* (PML) concept. Sim-

ilarly, Tekitek et al. [15], proposed a lattice Boltzmann scheme modeling the PML of Bérenger. Another approach was used by Izquierdo and Fueyo [16], who solved a system of differential equations and obtained a Dirichlet condition with non-reflecting properties. Their procedure is an approximate method to the *Navier-Stokes characteristic boundary condition* (NS-CBC) by Poinso and Lele [8]. This system contains only one dimensional information at the artificial boundaries, so their condition can be seen as an implementation of simplified Thompson’s boundary conditions where higher spatial derivatives are neglected. The aim of this work is to extend these known CBCs by Thompson [6] and the LBM application [16] in two respects: (a) inclusion of more spatial information (derivatives) at the artificial boundary and (b) enable possibly smaller reflection rates.

To this end, this article is structured as follows. In Section 2 we present a short introduction to the LBM and also explain briefly the construction of a boundary condition within this framework. Section 3 is devoted to a description of NRBCs. Here the conditions are described continuously and are therefore formulated independent of the used numerical method. Then, in Section 4 we explain how the boundary conditions of Section 3 are implemented within the fully discrete lattice Boltzmann context in two dimensions. In the last section we present our numerical results of three test cases for the NRBCs and finally we conclude.

2. The Lattice Boltzmann Method

The Boltzmann equation describes the evolution of the single particle distribution function $f(\vec{x}, \vec{\xi}, t)$:

$$\frac{\partial f(\vec{x}, \vec{\xi}, t)}{\partial t} + \vec{\xi} \cdot \nabla f(\vec{x}, \vec{\xi}, t) = Q(f),$$

in terms of the space coordinate $\vec{x} \in \mathbb{R}^d$, molecular velocity $\vec{\xi} \in \mathbb{R}^d$, time $t > 0$ and collision term $Q(f)$. From this microscopic description macroscopic quantities like the mass density ρ and the fluid velocity \vec{u} are obtained by computing moments of f .

The LBM can be regarded as a special discretization of the Boltzmann equation [17], where the molecular velocity space $\vec{\xi} \in \mathbb{R}^d$ is restricted to a finite set of given velocities $\vec{c}_i \in \mathbb{R}^d$, $i = 0, \dots, n_v$. Next, for a given time step size Δt the spatial discretization is obtained with the velocity set by $\Delta \vec{x} = \vec{c}_i \Delta t$.

That is, in the time period Δt particles move from one lattice site \vec{x} to a neighboring site $\vec{x} + \Delta\vec{x}$. Commonly, in LBM the Boltzmann collision integral $Q(f)$ is approximated by a relaxation towards the local equilibrium $f^{(\text{eq})}$. Here we use the popular BGK model [18], which is a single relaxation time model. This approach yields the following lattice Boltzmann equation [1]:

$$f_i(\vec{x} + \vec{c}_i \Delta t, t + \Delta t) - f_i(\vec{x}, t) = -\frac{\Delta t}{\tau} \left[f_i(\vec{x}, t) - f_i^{(\text{eq})}(\vec{x}, t) \right], \quad (1)$$

which is an evolution equation for the discrete particle distribution f_i (corresponding to \vec{c}_i). The right-hand side, with the free relaxation parameter τ , is the discrete BGK-model for $Q(f)$. The quantities $f_i(\vec{x}, t)$ are called *populations*. In this work, we consider two space dimensions with 9 ($n_v = 8$) lattice velocities (D2Q9 model):

$$\begin{aligned} \vec{c}_0 &= \vec{0}, & \vec{c}_i &= c \begin{pmatrix} \cos\left(\frac{\pi}{2}(i-1)\right) \\ \sin\left(\frac{\pi}{2}(i-1)\right) \end{pmatrix}, & i &= 1, 2, 3, 4, \\ \vec{c}_j &= c \begin{pmatrix} \sqrt{2} \cos\left(\frac{\pi}{2}(j-\frac{1}{2})\right) \\ \sqrt{2} \sin\left(\frac{\pi}{2}(j-\frac{1}{2})\right) \end{pmatrix}, & j &= 5, 6, 7, 8. \end{aligned}$$

Moreover, the local equilibrium $f_i^{(\text{eq})}$ is given by:

$$\begin{aligned} f_i^{(\text{eq})}(\vec{x}, t) &= w_i \rho(\vec{x}, t) \left[1 + \frac{3}{c^2} (\vec{c}_i \cdot \vec{u}(\vec{x}, t)) + \frac{9}{2c^4} (\vec{c}_i \cdot \vec{u}(\vec{x}, t))^2 - \frac{3}{2c^2} |\vec{u}(\vec{x}, t)|^2 \right] \quad (2) \end{aligned}$$

with the weights $w_0 = 4/9$, $w_{1-4} = 1/9$ and $w_{5-8} = 1/36$. The macroscopic quantities mass density and fluid velocity are computed in each lattice point by

$$\rho(\vec{x}, t) = \sum_{i=0}^8 f_i(\vec{x}, t), \quad \vec{u}(\vec{x}, t) = \frac{1}{\rho(\vec{x}, t)} \sum_{i=1}^8 \vec{c}_i f_i(\vec{x}, t). \quad (3)$$

These formulas represent discrete moments of f . The time evolution of the system (1) can be split into two parts (cf. Fig. 1): the collision part

$$\tilde{f}_i(\vec{x}, t) = f_i(\vec{x}, t) - \frac{\Delta t}{\tau} \left[f_i(\vec{x}, t) - f_i^{(\text{eq})}(\vec{x}, t) \right]$$

which are *compressible Navier-Stokes equations*. Furthermore, the Chapman-Enskog expansion relates the mass density and the pressure in LBM:

$$p(x, t) = c_s^2 \rho(x, t), \quad (6)$$

where $c_s = c/\sqrt{3}$ denotes the speed of sound in D2Q9. The relaxation time τ (in the BGK approximation) is linked to the kinematic viscosity ν via

$$\nu = \frac{\eta}{\rho} = \frac{2\tau - \Delta t}{6} c^2.$$

3. Characteristic Boundary Conditions

We will construct non-reflecting Dirichlet boundary conditions for the mass density and the fluid velocity. To this end, the characteristics of a nonlinear hyperbolic system at the boundary are analyzed. Therefore one refers to this type of boundary conditions as characteristic boundary conditions (CBCs). The underlying hyperbolic system is obtained from (5) by dropping the Laplacian [6], i.e., the resulting momentum equation lacks a viscosity term and equals the momentum equation of the Euler equations. Further, as a simplification of [6], we drop the energy equation and finally obtain for the characteristic variables $\vec{U}^\top = (\rho, v, w)$:

$$\frac{\partial \vec{U}}{\partial t} + A \frac{\partial \vec{U}}{\partial x} + B \frac{\partial \vec{U}}{\partial y} = 0, \quad (7)$$

with the coefficient matrices

$$A = A(\rho, v, w) = \begin{pmatrix} v & \rho & 0 \\ \frac{c_s^2}{\rho} & v & 0 \\ 0 & 0 & v \end{pmatrix}, \quad B = B(\rho, v, w) = \begin{pmatrix} w & 0 & \rho \\ 0 & w & 0 \\ \frac{c_s^2}{\rho} & 0 & w \end{pmatrix}.$$

Here v and w denote the velocity in x and y direction, respectively. As (7) is a hyperbolic system, the coefficient matrices are (real) diagonalizable

$$SAS^{-1} = \Lambda, \quad TBT^{-1} = M, \quad (8)$$

with suitable matrices S , T and diagonal matrices of eigenvalues:

$$\begin{aligned} \Lambda &= \text{diag}(\lambda_1, \lambda_2, \lambda_3) = \text{diag}(v - c_s, v, v + c_s), \\ M &= \text{diag}(\mu_1, \mu_2, \mu_3) = \text{diag}(w - c_s, w, w + c_s). \end{aligned}$$

One choice is

$$\begin{aligned}
 S &= \begin{pmatrix} c_s^2 & -c_s\rho & 0 \\ 0 & 0 & 1 \\ c_s^2 & c_s\rho & 0 \end{pmatrix}, & S^{-1} &= \begin{pmatrix} \frac{1}{2c_s^2} & 0 & \frac{1}{2c_s^2} \\ -\frac{1}{2c_s\rho} & 0 & \frac{1}{2c_s\rho} \\ 0 & 1 & 0 \end{pmatrix}, \\
 T &= \begin{pmatrix} c_s^2 & 0 & -c_s\rho \\ 0 & 1 & 0 \\ c_s^2 & 0 & c_s\rho \end{pmatrix}, & T^{-1} &= \begin{pmatrix} \frac{1}{2c_s^2} & 0 & \frac{1}{2c_s^2} \\ 0 & 1 & 0 \\ -\frac{1}{2c_s\rho} & 0 & \frac{1}{2c_s\rho} \end{pmatrix}.
 \end{aligned}$$

Now we can separate in- and outgoing waves by inspecting the eigenvalues and associated eigenvectors. While the outgoing waves can be solved from the given interior information, this is not possible for incoming waves. If available, an exterior solution can be used to specify the incoming waves.

As proposed by Hedstrom [5] and Thompson [6], non-reflecting boundary conditions (NRBCs) are based on annihilating the incoming waves. To explain this approach in more detail, we consider an x -boundary (a boundary with $x = \text{const.}$) for the system (7). The spatial derivatives perpendicular to the boundary are expressed in characteristic coordinates using (8):

$$A \frac{\partial \vec{U}}{\partial x} = S^{-1} \Lambda S \frac{\partial \vec{U}}{\partial x} =: S^{-1} \vec{\mathcal{L}}_x, \quad \vec{\mathcal{L}}_x = \begin{pmatrix} \mathcal{L}_{x,1} \\ \mathcal{L}_{x,2} \\ \mathcal{L}_{x,3} \end{pmatrix}.$$

Hereby the components $\mathcal{L}_{x,i} = \lambda_i \vec{\ell}_i^\top \frac{\partial \vec{U}}{\partial x}$ express the amplitude variations of the characteristic waves [8] ($\vec{\ell}_i^\top$ denotes the i th row of S). The sign of λ_i (characteristic speed) indicates the direction of the wave: a positive eigenvalue corresponds to a wave traveling in positive x -direction and vice versa. Following the idea of Hedstrom [5] and Thompson [6] incoming waves are annihilated by simply setting the corresponding wave amplitude variations to zero, that is,

$$\tilde{\mathcal{L}}_{x,i} = \begin{cases} \lambda_i \vec{\ell}_i^\top \frac{\partial \vec{U}}{\partial x} & \text{for an outgoing wave} \\ 0 & \text{for an incoming wave.} \end{cases} \quad (9)$$

In the sequel we present three corresponding variants of this NRBCs.

3.1. Thompson’s Non-Reflecting Boundary Conditions

In the NRBC by Thompson [6], the Dirichlet values for the characteristic variables are obtained by solving

$$\frac{\partial \vec{U}}{\partial t} + B \frac{\partial \vec{U}}{\partial y} = -S^{-1} \vec{\mathcal{L}}_x \quad (10)$$

on the boundary with $\vec{\mathcal{L}}_x$ obtained from (9).

3.2. Local One-Dimensional Inviscid Equations (LODI)

Izquierdo and Fueyo [16] presented NRBCs for the LBM based on the NS-CBC developed by Poinso and Lele [8]. They solve the so-called *local one-dimensional inviscid* (LODI) equations on the boundary, and annihilate the incoming waves described within the LODI framework. For an x -boundary, this procedure is equivalent to solve:

$$\frac{\partial \vec{U}}{\partial t} = -S^{-1} \vec{\mathcal{L}}_x. \quad (11)$$

3.3. Modified Thompson Boundary Condition

By inspecting carefully the errors of Thompson’s and the LODI approach, we observed that Thompson’s boundary condition overestimated certain quantities and at the same time the LODI approach underestimated them. These related quantities are the velocity tangential to the boundary and the mass density. This numerical evidence gives us the motivation to construct a new method by taking in each time step a convex combination of both methods, i.e., solving the system

$$\frac{\partial \vec{U}}{\partial t} + \gamma B \frac{\partial \vec{U}}{\partial y} = -S^{-1} \vec{\mathcal{L}}_x, \quad (12)$$

where $\gamma \in [0, 1]$ is a free parameter. This procedure is referred to as *modified Thompson Boundary Condition* (ModThom) and the corresponding values \vec{U}_{ModThom} can be interpreted as convex combinations

$$\vec{U}_{\text{ModThom}} = \gamma \vec{U}_{\text{Thom}} + (1 - \gamma) \vec{U}_{\text{LODI}},$$

where \vec{U}_{Thom} and \vec{U}_{LODI} are solutions obtained from (10) and (11), respectively. Thus, it is a generalization of the two previous methods.

3.4. The Treatment of Corners

A characteristics analysis can be done in both directions [6]. That is, in addition to the description above (the one for an x -boundary) we also express the y -derivatives in characteristics

$$B \frac{\partial \vec{U}}{\partial y} = T^{-1} M T \frac{\partial \vec{U}}{\partial y} =: T^{-1} \vec{\mathcal{L}}_y, \quad \vec{\mathcal{L}}_y = \begin{pmatrix} \mathcal{L}_{y,1} \\ \mathcal{L}_{y,2} \\ \mathcal{L}_{y,3} \end{pmatrix}.$$

Again, we set the wave amplitude variations corresponding to incoming waves to zero:

$$\tilde{\mathcal{L}}_{y,i} = \begin{cases} \mu_i \vec{m}_i^\top \frac{\partial \vec{U}}{\partial y} & \text{for an outgoing wave,} \\ 0 & \text{for an incoming wave,} \end{cases}$$

where \vec{m}_i^\top is the i th row of T . Hence, for a corner we solve the system of ordinary differential equations (ODEs):

$$\frac{\partial \vec{U}}{\partial t} = -S^{-1} \vec{\mathcal{L}}_x - T^{-1} \vec{\mathcal{L}}_y.$$

This procedure for handling corners is the same for all CBCs described above.

4. 2D Characteristic Boundary Conditions in LBM

Next, we describe certain important details of the implementation. In the description, the goal is to proceed from a time level t_0 to $t_1 = t_0 + \Delta t$ for all populations and macroscopic variables at the boundary. This computation can be split into three steps. First, the wave amplitude variations are calculated. Then the differential equations (on the boundary) are solved by time integration. Finally, the results of the time integration are transferred to the populations.

4.1. Step 1: Computation of Wave Amplitude Variations

For all CBCs introduced above the wave amplitude variations are given by (9) for an x -boundary. In detail they read:

$$\tilde{\mathcal{L}}_{x,1} = \begin{cases} (v - c_s) [c_s^2 \frac{\partial \rho}{\partial x} - c_s \rho \frac{\partial v}{\partial x}] & \text{for an outgoing wave,} \\ 0 & \text{for an incoming wave,} \end{cases}$$

$$\tilde{\mathcal{L}}_{x,2} = \begin{cases} v \frac{\partial w}{\partial x} & \text{for an outgoing wave,} \\ 0 & \text{for an incoming wave,} \end{cases}$$

$$\tilde{\mathcal{L}}_{x,3} = \begin{cases} (v + c_s) \left[c_s^2 \frac{\partial \rho}{\partial x} + c_s \rho \frac{\partial v}{\partial x} \right] & \text{for an outgoing wave,} \\ 0 & \text{for an incoming wave.} \end{cases}$$

The appearing derivatives perpendicular to the boundary are approximated by one-sided second order finite difference quotients:

$$\frac{\partial z}{\partial x}(x_0) = \frac{1}{2} \left(-3z(x_0) + 4z(x_1) - z(x_2) \right).$$

This gives numerical approximations $\tilde{\mathcal{L}}_{x,i}^{\text{FD}}$, which are inserted into the right hand sides of the differential equations (10), (11) and (12):

$$-S^{-1} \vec{\mathcal{L}}_x^{\text{FD}} = \begin{pmatrix} -\frac{1}{2c_s^2} \left(\tilde{\mathcal{L}}_{x,1}^{\text{FD}} + \tilde{\mathcal{L}}_3^{\text{FD}} \right) \\ \frac{1}{2c_s \rho} \left(\tilde{\mathcal{L}}_{x,1}^{\text{FD}} - \tilde{\mathcal{L}}_{x,3}^{\text{FD}} \right) \\ -\tilde{\mathcal{L}}_{x,2}^{\text{FD}} \end{pmatrix}.$$

4.2. Step 2: Time Integration at the Boundary

The ODE (11) is solved for simplicity by using one explicit Euler step. For the PDEs (10) and (12) the spatial derivatives are discretized first. Here a second order centered finite difference stencil is applied:

$$\frac{\partial z}{\partial y}(y_1) = \frac{1}{2} \left(z(y_2) - z(y_0) \right).$$

In case of Thompson's boundary condition, the resulting ODE is solved by two different methods in our numerical tests below. By *Thom-1* we denote the integration with one explicit Euler step. And by *Thom-2*, we denote the explicit scheme proposed by Thompson [6]: (a 2nd order RK-method, which is 4th order for linear systems)

$$\begin{aligned} \vec{U}(t_{1/4}) &= \vec{U}(t_0) - \frac{\Delta t}{4} \left(B \frac{\partial \vec{U}}{\partial y}(t_0) + S^{-1} \vec{\mathcal{L}}_x^{\text{FD}} \right), \\ \vec{U}(t_{1/3}) &= \vec{U}(t_0) - \frac{\Delta t}{3} \left(B \frac{\partial \vec{U}}{\partial y}(t_{1/4}) + S^{-1} \vec{\mathcal{L}}_x^{\text{FD}} \right), \\ \vec{U}(t_{1/2}) &= \vec{U}(t_0) - \frac{\Delta t}{2} \left(B \frac{\partial \vec{U}}{\partial y}(t_{1/3}) + S^{-1} \vec{\mathcal{L}}_x^{\text{FD}} \right), \\ \vec{U}(t_1) &= \vec{U}(t_0) - \Delta t \left(B \frac{\partial \vec{U}}{\partial y}(t_{1/2}) + S^{-1} \vec{\mathcal{L}}_x^{\text{FD}} \right). \end{aligned}$$

The wave amplitude variations are computed only once. The modified Thompson boundary condition is implemented using one explicit Euler step.

4.3. Step 3: Transfer to LBM

Let the Dirichlet values obtained in the previous step be denoted as ρ_D , v_D and w_D . For a boundary lattice point \vec{x}_B the populations $f_i(\vec{x}_B)$ have to be computed. As described above, equilibrium boundary conditions (EBCs) are a simple choice:

$$\begin{aligned} f_i(\vec{x}_B, t_1) &= f_i^{(\text{eq})}(\vec{x}_B) \\ &= w_i \rho_D(\vec{x}_B) \left[1 + \frac{3}{c^2} (\vec{c}_i \cdot \vec{u}_D(\vec{x}_B)) + \frac{9}{2c^4} (\vec{c}_i \cdot \vec{u}_D(\vec{x}_B))^2 - \frac{3}{2c^2} |\vec{u}_D(\vec{x}_B)|^2 \right], \end{aligned}$$

where $\vec{u}_D(\vec{x}_B) = (v_D(\vec{x}_B), w_D(\vec{x}_B))^\top$. This implementation is independent of the location of the boundary.

In the mEBC implementation, the non-equilibrium part is linearly extrapolated. Let $n_i(\vec{x}) = f_i(\vec{x}) - f_i^{(\text{eq})}(\vec{x})$ denote the non-equilibrium part at an interior lattice point. Then the mEBC assigns the populations at a boundary lattice point \vec{x}_B as:

$$f_i(\vec{x}_B, t_1) = f_i^{(\text{eq})}(\vec{x}_B, t_1) + 2n_i(\vec{x}_{B+1}, t_1) - n_i(\vec{x}_{B+2}, t_1),$$

where \vec{x}_{B+1} and \vec{x}_{B+2} refer to the next interior lattice points in the normal direction to the boundary. For a corner lattice point we assume the normal direction to be the diagonal. Note that the non-equilibrium parts of interior lattice points can be computed at the new time level, since all information required are known after the transport step.

5. Numerical Results

Three simple test cases are presented in the following. First, a plane wave with several orientations is simulated to test the accuracy of the CBCs for different angles of incidence. In the second test case, different angles are combined in one simulation where a two dimensional pressure wave is simulated. In both test cases, there are at most two sides of the rectangular domain equipped with NRBCs. In the third case, we test the long time behavior of the boundary conditions. Here we simulate again a two dimensional pressure wave, but this time the domain supplied with four non-reflecting boundaries. In the first and second test case we used $\gamma = 0.75$.

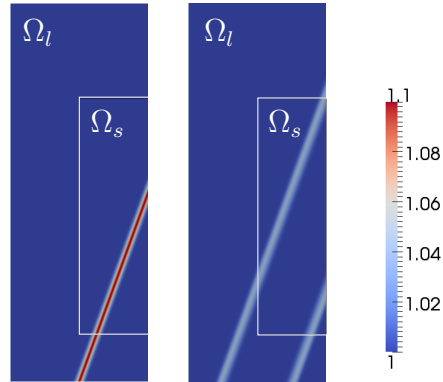


Figure 2: Left: Initial state for plane wave with $\varphi = 20^\circ$. Right: The state when the boundary condition is switched from exact one (using values from Ω_l) to a NRBC.

5.1. First Test Case: Plane Wave

A plane wave is simulated, which reaches the boundary with an angle of incidence φ . At $t = 0$, we initialize the fluid in the equilibrium state with zero velocity and a mass density computed according to the plane wave pressure profile:

$$p(x, y) = p_0 + (p_{\max} - p_0) \exp\left(\frac{-\hat{x}(x, y)^2}{2s^2}\right).$$

Here the transformed locations read

$$\begin{pmatrix} \hat{x}(x, y) \\ \hat{y}(x, y) \end{pmatrix} = \begin{pmatrix} \cos(\varphi \frac{\pi}{180}) & -\sin(\varphi \frac{\pi}{180}) \\ \sin(\varphi \frac{\pi}{180}) & \cos(\varphi \frac{\pi}{180}) \end{pmatrix}^{-1} \begin{pmatrix} x \\ y \end{pmatrix}.$$

Furthermore, we have chosen $s = 1/50$, $\rho_0 = 1$ and $\rho_{\max} = 1.1$, which yield the required pressure values according to (6).

The general case $\varphi > 0^\circ$: To test the NRBCs, a small domain Ω_s is described by a lattice of dimension $300 \times n_y$, where n_y depends on φ : $n_y = 300/\tan(\varphi)$. For angles $0^\circ < \varphi \leq 45^\circ$, we use the left boundary of Ω_s to test the NRBC, and for angles $45^\circ < \varphi < 90^\circ$ the upper boundary is used. To get rid of all other boundary effects, we embed the small domain of interest Ω_s into a larger domain Ω_l , see Fig. 2, and pre-simulate the corresponding problem on Ω_l . The results of that simulation are evaluated on $\partial\Omega_s$ and used as boundary conditions for all boundaries until the plane wave has completely reached the boundary, see Fig. 2 (right). Then the corresponding boundary condition (called 'exact') is switched to the chosen NRBC of Section 3.

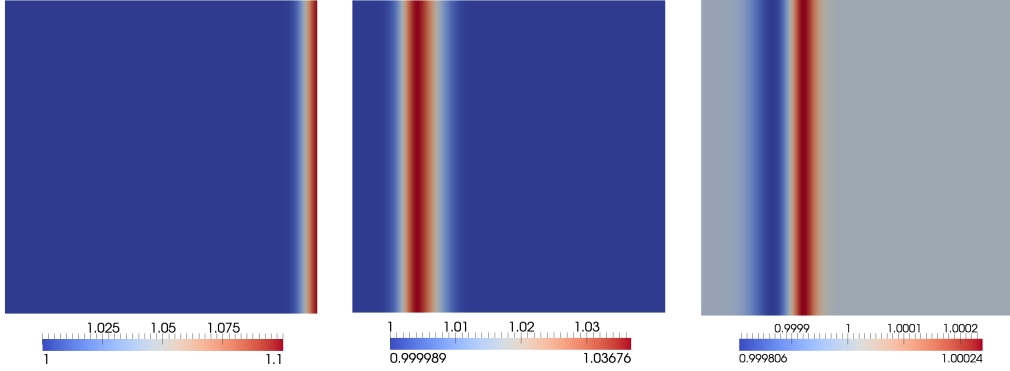


Figure 3: a) Initial state for plane wave with incidence angle $\varphi = 0^\circ$. b) Pressure wave moving towards the boundary. c) Reflected wave (LODI) moving away from the boundary.

Special case $\varphi = 0^\circ$: A square lattice of size 300×300 is used for the case $\varphi = 0^\circ$. The pressure wave is initialized axisymmetrically to the right boundary, see Fig. 3. We use periodic boundary conditions for the upper and lower boundary. On the right boundary we use a boundary condition emulating the line symmetry. For the left boundary the NRBC is selected.

Evaluation of results: The reflection coefficient $r(\varphi)$ of the boundary conditions is measured by computing the ratio of maximal amplitudes (in the density waves):

$$r(\varphi) = \frac{|R|}{|I|},$$

where the amplitude of the unphysical reflected density wave is R and the amplitude of the original density wave running towards the boundary is I . The reflection coefficient is plotted for several angles of incidence in Fig. 4. The maximal amplitude I is independent of the boundary condition, thus a smaller value of the error ratio r is equivalent to less unphysical reflection. By inspecting the plot in Fig. 4 we observe that the reflection of Thompson’s boundary condition is a little smaller than the one of the LODI approach. The unphysical reflections can be reduced significantly when using the modified Thompson boundary condition. Our numerical tests showed the best results for $\gamma = 0.75$.

5.2. Second Test Case: Concentric Waves

This test case is performed on a 900×1600 lattice representing the rectangle $\Omega_s = [-0.9, 0.9] \times [-1.6, 1.6]$. The fluid is initialized at rest with a Gaussian

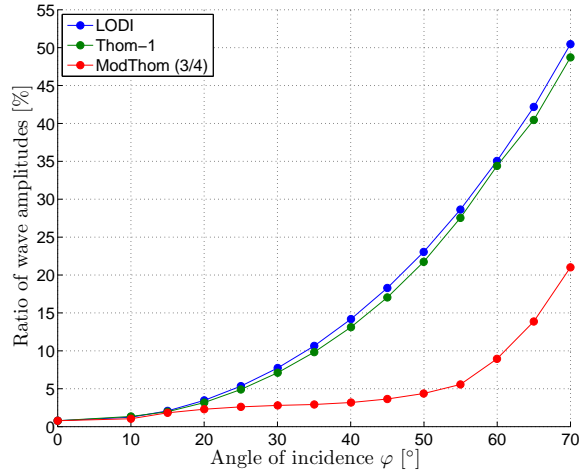


Figure 4: The reflection coefficient $r(\varphi)$ of CBCs when simulating plane waves depending on the angles of incidence. The data is linearly interpolated.

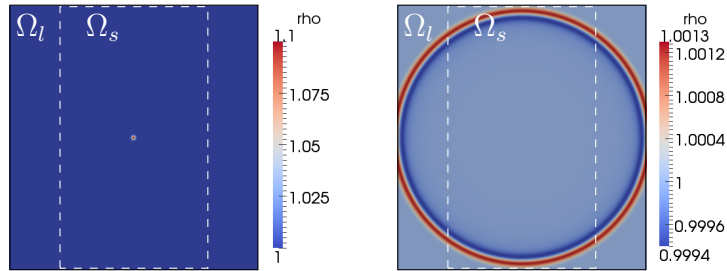


Figure 5: The computational domain of the second test case with initial state (left) and final state (right).

pressure perturbation having its peak in the center:

$$p(x, y) = p_0 + (p_{\max} - p_0) \exp\left(\frac{-(x^2 + y^2)}{2s^2}\right). \quad (13)$$

As above, we set $\rho_0 = 1$ and $\rho_{\max} = 1.1$, then the required pressure values follow from (6). Moreover we have chosen $s = 1/60$. On the left and right side of Ω_s NRBCs are supplied. For the upper and lower boundaries we considered periodic boundary conditions. A reference solution on Ω_s with exact NRBCs was achieved by a simulation on a significantly larger domain $\Omega_l \supset \Omega_s$ with lattice size 1500×1600 , see Fig. 5. The reference results obtained on the larger domain Ω_l are marked with a bar. We simulated 1300

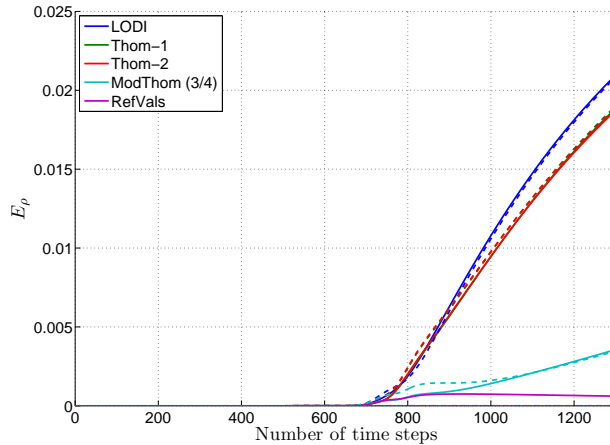


Figure 6: The evolution of the error E_ρ for different boundary conditions, using EBC (solid) and mEBC (dashed) approach for the transfer of Dirichlet values to LBM.

time steps, such that the wave did not reach the upper and lower boundary, see Fig. 5 (right).

We compute for different time levels the errors caused by the implemented boundary condition on Ω_s :

$$E_z = \sqrt{\sum_{\vec{x} \in \Omega_s} \left(z(\vec{x}) - \bar{z}(\vec{x}) \right)^2} \quad \text{with } z \in \{\rho, u, w\}.$$

If the obtained values $\bar{\rho}$, \bar{v} and \bar{w} from the simulation on the larger domain Ω_l were used as Dirichlet values on Ω_s , also an error would be created due to EBC. Therefore these results serve us as reference values (*RefVals*). This error can be reduced significantly by using mEBC instead. To measure only these deviations, we use the following error norms:

$$D_\rho^2 = \sqrt{\sum_{\vec{x} \in \partial\Omega_s^W} \left(\rho(\vec{x}) - \bar{\rho}(\vec{x}) \right)^2}, \quad D_\rho^\infty = \max_{\vec{x} \in \partial\Omega_s^W} \{ |\rho(\vec{x}) - \bar{\rho}(\vec{x})| \},$$

(in the Dirichlet values at different time levels), where the left boundary (at $x_1 = -0.9$) is abbreviated by $\partial\Omega_s^W$. Analogously, D_v^2 , D_v^∞ , D_w^2 and D_w^∞ are defined. The errors E_ρ , E_v and E_w are plotted in Figs. 6–7. We observe that Thom-1 and Thom-2 yield very similar results. Moreover, using mEBC only results in a significant change for ModThom and RefVals. The modified

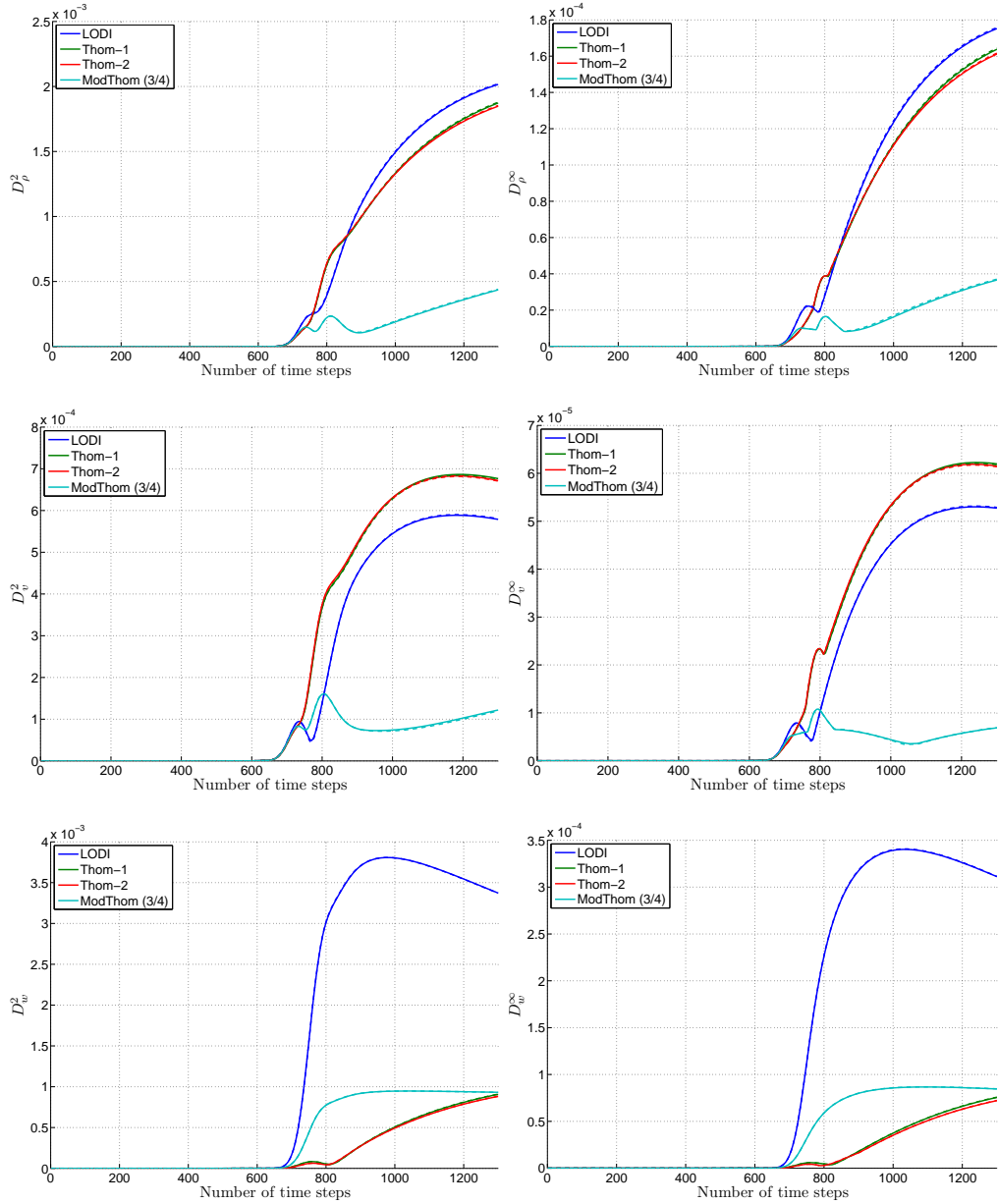


Figure 8: The evolution of D_ρ^2 (upper left), D_ρ^∞ (upper right), D_v^2 (middle left), D_v^∞ (middle right), D_w^2 (lower left) and D_w^∞ (lower right) for different boundary conditions, using EBC (solid) and mEBC (dashed) approach for the transfer of Dirichlet values to LBM.

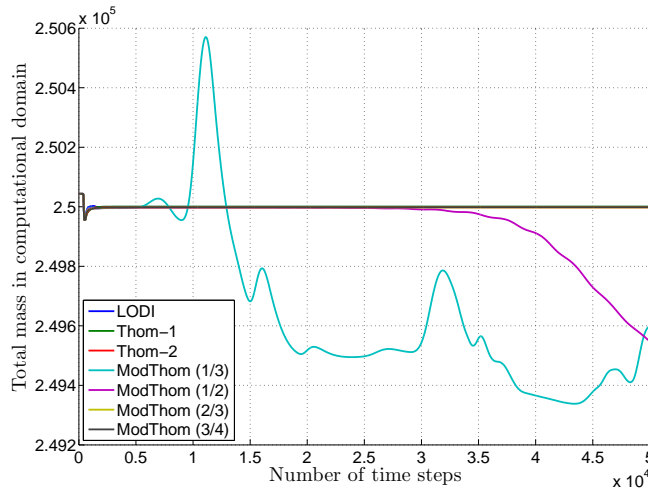


Figure 9: The total mass for different boundary conditions.

ferent boundary conditions; we picked $\gamma = 1/3$ and $\gamma = 0.5$ as two examples of unstable conditions.

6. Conclusions

Artificial boundaries need suitable computational conditions to close the mathematical model, but they shall not induce unphysical effects into the solutions. We considered a couple of simulation test cases from fluid dynamics and we proposed two novel NRBCs for the LBM. To this end, we described the well-known NRBCs of Thompson [6] concisely and tailored to our purpose, i.e., without an energy equation. Then we transferred these results to NRBCs for the LBM. To the best of the authors' knowledge, this was done here for the first time and it extends the LODI approach [8] to include higher space dimensions. Furthermore, a modified boundary condition was developed showing a much smaller error in all our numerical test cases. We observed that the free parameter in the modified boundary condition had a key impact on the long time stability.

As further perspective, we aim at finding an analytical verification for the numerical long time instability caused by some choices of this free parameter. Also we like to investigate the optimal choices for the parameter.

- [1] S. Chen, G. D. Doolen, Lattice Boltzmann method for fluid flows, *Ann Rev Fluid Mech* 30 (1) (1998) 329–364.

- [2] S. Succi, *The lattice Boltzmann Equation for fluid dynamics and beyond*, Oxford University Press, Oxford, UK, 2001.
- [3] D. Heubes, A. Bartel, M. Ehrhardt, *An Introduction to Lattice-Boltzmann Methods*, Chapter 1 in: M. Ehrhardt (ed.), *Novel Trends in Lattice-Boltzmann Methods - Reactive Flow*, Physicochemical Transport and Fluid-Structure Interaction, Progress in Computational Physics, Vol. 3, Bentham Science Publishers Ltd., to appear 2013.
- [4] B. Engquist, A. Majda, Absorbing boundary conditions for the numerical simulation of waves, *Math Comput* 31 (1977) 629–651.
- [5] G. W. Hedstrom, Nonreflecting boundary conditions for nonlinear hyperbolic systems, *J Comput Phys* 30 (2) (1979) 222–237.
- [6] K. W. Thompson, Time dependent boundary conditions for hyperbolic systems, *J Comput Phys* 68 (1) (1987) 1–24.
- [7] D. Kröner, Absorbing boundary conditions for the linearized Euler equations in 2-D, *Math Comput* 57 (195) (1991) 153–167.
- [8] T. Poinso, S. Lele, Boundary conditions for direct simulations of compressible viscous flows, *J Comput Phys* 101 (1) (1992) 104–129.
- [9] J. Wilson, Derivation of boundary conditions for the artificial boundaries associated with the solution of certain time dependent problems by Lax–Wendroff type difference schemes, *Proc Edinb Math Soc*, II. Ser. 25 (1982) 1–18.
- [10] C. Rowley, T. Colonius, Discretely nonreflecting boundary conditions for linear hyperbolic systems, *J Comput Phys* 157 (2000) 500–538.
- [11] M. Ehrhardt, Absorbing boundary conditions for hyperbolic systems, *Numer Math Theor Meth Appl* 3 (2010) 295–337.
- [12] T. Amro, A. Arnold, M. Ehrhardt, Optimized far field boundary conditions for hyperbolic systems, Preprint BUW-IMACM 12/02, University of Wuppertal, January 2012.
- [13] E.W.S. Kam, R.M.C. So, R.C.K. Leung, Lattice Boltzmann method simulation of aeroacoustics and nonreflecting boundary conditions, *AIAA* 45 (7) (2007), 1703–1712.

- [14] A. Najafi-Yazdi, L. Mongeau, An absorbing boundary condition for the lattice Boltzmann method based on the perfectly matched layer, *Comput Fluids* 68 (2012) 203–218.
- [15] M. Tekitek, M. Bouzidi, F. Dubois, P. Lallemand, Towards perfectly matching layers for lattice Boltzmann equation, *Comput Math Appl* 58 (5) (2009) 903–913.
- [16] S. Izquierdo, N. Fueyo, Characteristic nonreflecting boundary conditions for open boundaries in lattice Boltzmann methods, *Phys Rev E* 78 (2008) 046707.
- [17] X. He, L.-S. Luo, Theory of the lattice Boltzmann method: From the Boltzmann equation to the lattice Boltzmann equation, *Phys Rev E* 56 (6) (1997) 6811–6817.
- [18] P. L. Bhatnagar, E. P. Gross, M. Krook, A model for collision processes in gases. I. Small amplitude processes in charged and neutral one-component systems, *Phys Rev* 94 (3) (1954) 511–525.
- [19] T. Inamuro, M. Yoshino, F. Ogino, A non-slip boundary condition for lattice Boltzmann simulations, *Phys Fluids* 7 (1995) 2928–2930.
- [20] Q. Zou, X. He, On pressure and velocity boundary conditions for the lattice Boltzmann BGK model, *Phys Fluids* 9 (6) (1997) 1591–1598.
- [21] S. Chapman, T. Cowling, *The mathematical theory of non-uniform gases*, Cambridge University Press, London, UK, 1970.